Microstructure Characterization and Constitutive Modelling of Waterborne Epoxy Resin Modified Bitumen Emulsion

Rui Li [a], Zhen Leng [a*], Haopeng Wang [b], Manfred N. Partl [c], Huayang Yu [d], Zhifei Tan [a], Christiane Raab [c]

[a] *Department of Civil and Environmental Engineering, The Hong Kong Polytechnic University, Hong Kong SAR, China*

[b] *Section of Pavement Engineering, Faculty of Civil Engineering & Geosciences, Delft University of Technology, Netherland*

[c] *Laboratory of Road Engineering, Empa Swiss Federal Laboratories for Materials Science and Technology, Dübendorf, Switzerland*

[d] *School of Civil Engineering and Transportation, South China University of Technology, Guangzhou, China*

* Corresponding author: zhen.leng@polyu.edu.hk (Z. Leng)

Microstructure Characterization and Constitutive Modelling of Waterborne Epoxy Resin Modified Bitumen Emulsion

Abstract: From the pavement construction emission perspective, bitumen emulsion is considered more environment-friendly than conventional bitumen, because of its much lower construction temperature. However, bitumen emulsion faces the major concern of low mechanical strength especially at high service temperatures. To improve the mechanical performance of bitumen emulsion, waterborne epoxy resin can be used as a modifier. Nevertheless, there still lacks fundamental understanding on the effects of waterborne epoxy resin on the microstructure and rheological performances of the residual bitumen of the emulsion. To fill this gap, this study aims to investigate the microstructure and develop the constitutive model of the waterborne epoxy resin modified bitumen emulsion residue (WEBER). To achieve this objective, a confocal laser scanning microscopy (CLSM) was first adopted to characterize the microstructure of WEBER. The frequency sweep tests were then conducted, and the '2S2P1D' model was applied to simulate the WEBER's dynamic response at different loading frequencies. The results indicated that the waterborne epoxy resin formed a polymer-rich film around the bitumen phase in the emulsion residue when its content reached 3wt%, and the '2S2P1D' model can well describe the WEBER's dynamic response at different loading frequencies.

Key words: Bitumen emulsion; Waterborne epoxy resin; Microstructure; Constitutive relation; '2S2P1D' model

1 Introduction

Bituminous mixture is the major type of material used to pave the roads worldwide. Due to the comparatively high viscosity of bitumen binder at room temperature, the bituminous mixture must be mixed and constructed at high temperature to improve its workability, which leads to inevitable short-term aging of the binder (Calabi-Floody and Thenoux, 2012, Mirwald et al., 2020, Edwards et al., 2005). The aging of bitumen involves a series of complex physicochemical process that leads to change of composition and increase of polarity (Lu and Isacsson, 2000, Nivitha et al., 2016). Previous studies indicate that aging typically reduced the low temperature performance and fatigue resistance of bitumen, due to

increasing brittleness of the binder after aging (Raad et al., 2001, Kim and Lee, 2003). In addition, the high-temperature mixing and application may produce significant amount of volatile organic compounds (VOCs) and greenhouse gases (GHGs), thereby affecting the environment and human health (Capitão et al., 2012). Bitumen emulsion, on the other hand, can be directly applied without heating because of its low viscosity at room temperature, significantly reducing energy consumption and hazardous emissions. However, bitumen emulsion faces the major concern of low mechanical strength, especially at high service temperatures (Gómez-Meijide and Pérez, 2014, Li et al., 2020). To improve the mechanical performance of bitumen emulsion, polymer latexes such as styrene butadiene rubber (SBR) latex, natural rubber (NR) latex and chloroprene rubber (CR) latex have been commonly used (Khadivar and Kavussi, 2013, Takamura, 2002, Jiang et al., 2020). Recently, waterborne epoxy resin has emerged as a novel modifier for bitumen emulsion, which was found effective in improving the mechanical performance of bitumen emulsion (Li et al., 2019, Li et al., 2021, Hu et al., 2019). However, the effects of waterborne epoxy resin on the microstructure and viscoelastic behavior of the residual bitumen have not been fully understood yet.

Polymers have been commonly used to improve the viscoelastic properties of bitumen. The macroscopic viscoelastic behavior of polymer modified bitumen (PMB) depends highly on its microstructure, i.e., the distribution of polymer in PMB. The fluorescence microscopy is frequently used to visually inspect the microstructure of PMB (Zhu et al., 2018). Previous studies indicated that a continuous polymer-rich phase can be observed when the polymer content reaches 6-7wt% (Topal, 2010), i.e., the phase inversion point of PMB. In contrast, it is reported by Forbes et al. (2001) that the phase inversion potin of the SBR latex modified bitumen emulsion is about 3wt%, which is significantly smaller than that of PMB. Takamura's study on SBR modified bitumen emulsion revealed that the SBR latex was

dispersed in the aqueous phase and able to form a continuous polymer film around the bitumen phase upon the curing of the emulsion (Takamura, 2002). The above-mentioned polymers are generally thermoplastic based, which will melt when heated above certain temperature. On the other hand, the epoxy resin is a thermoset polymer, which forms an inter-connected polymer structure after the curing reaction and will not melt at higher temperature (Yamasaki and Morita, 2014, Dębska and Lichołai, 2016). How will the thermoset waterborne epoxy resin affect the microstructure and viscoelastic behaviour of WEBER is still not clear. Currently, there are very few studies on the microstructure of waterborne epoxy resin modified bitumen emulsion residue (WEBER), which may provide fundamental information for understanding the modification mechanism of waterborne epoxy resin and explaining the viscoelastic behaviour of WEBER.

Apart from various rheological experiments, different models have been developed to study the viscoelastic performance of bituminous materials, including the empirical algebraic and analogical models. The empirical algebraic models are mathematical formulations developed through fitting the experimental data, but the parameters may not have any physical meanings. On the other hand, the analogical models use different combinations of the elastic springs, viscous dashpots and/or parabolic viscous elements to simulate the viscoelastic behavior of bitumens. Some commonly used analogical models include the generalized Maxwell model, the generalized Kelvin-Voigt model, the Huet-Sayegh (HS) model, and the '2S2P1D' (two springs, two parabolic dashpots, and one linear dashpot) model (Olard and Di Benedetto, 2003). The generalized Maxwell model is composed of a number of parallel Maxwell models, while the generalized Kelvin-Voigt model is composed of a number of Kelvin-Voigt model in series. These two models can generally describe the viscoelastic properties of bitumen binders and mixtures fairly well as long as sufficient numbers of elements are adopted. However, their limitations are that many parameters are needed to fit the models, and the

models are discrete. In contrast, the Huet model (Huet, 1965), constituted by a spring and two parabolic dashpots in series, has a continuous spectrum, i.e., can be represented by an infinity number of Maxwell elements in parallel or Kelvin-Voigt elements in series. The original Huet model, however, lacks the ability in fitting PMB correctly. To overcome this limitation, Sayegh modified the Huet model by placing a spring in parallel with the Huet model, which resulted the Huet-Sayegh (HS) model (Sayegh, 1967). However, the accuracy of this model in fitting the rheological behavior of PMB at very low frequency is still limited (Olard and Di Benedetto, 2003). In this regard, Olard and Di Benedetto (2003) developed the so-called '2S2P1D' model by placing a linear dashpot in series with the parabolic elements and the spring of rigidity in the original HS model. It has been found that the '2S2P1D' model can simulate the viscoelastic responses of both bituminous binders and mixtures with high accuracy in a wide spectrum of frequency. In addition, the '2S2P1D' model has only 7 parameters, significantly less than those of the generalized Maxwell model and the generalized Kevin-Voigt model.

The performances of WEBER, such as the bonding property with aggregate, moisture sensitivity, and resistance to rutting and fatigue, have been investigated in a previous study (Li et al., 2019). This research mainly aims to characterize the microstructure and develop the constitutive model of WEBER, and investigate their relationship. To achieve this objective, the infrared spectra and the microstructure of WEBER were first characterized using the attenuated total reflection - Fourier transform infrared spectroscopy (ATR-FTIR) and confocal laser scanning microscopy (CLSM), respectively. The frequency sweep tests from 0.1Hz to 30Hz at temperatures of -10 °C to 60 °C were then conducted to measure the bulk rheological performance. Because of its accuracy in simulating the viscoelastic behavior of bituminous materials in a wide spectrum of frequency, the '2S2P1D' model was adopted to fit the complex modulus in the frequency domain.

2 Materials and Methods

2.1 Preparation of Waterborne Epoxy Resin Modified Bitumen Emulsion

The preparation of waterborne epoxy resin modified bitumen emulsion followed the same procedure adopted in one of our previous studies (Li et al., 2021). The waterborne epoxy resin emulsion was first prepared by mixing waterborne curing agent with epoxy resin based on stoichiometric amount, and the solid content was 60wt%. A base bitumen with a penetration grade of 60/70 (Pen 60/70) was used to prepare the cationic bitumen emulsion with a solid content of 63.0wt%. The basic properties of the bitumen emulsion are presented in Table 1. The epoxy resin emulsion was then mixed with bitumen emulsion for about 5 min to prepare the waterborne epoxy resin modified bitumen emulsion. Note that both the epoxy resin emulsion and the bitumen emulsion were cationic type to ensure compatibility of the two. To prepare WEBER, a thin layer of waterborne epoxy resin modified bitumen emulsion was maintained at ambient room condition for 3 days, followed by 24 h of oven conditioning at 60 °C. Such procedure was adopted to ensure complete curing of the waterborne epoxy resin. Figure 1 presents the detailed procedure for preparing the WEBER. Waterborne epoxy modified bitumen emulsion with three waterborne epoxy resin contents, 1wt%, 3wt%, and 5wt% based on the mass of the residual bitumen, were prepared, and they are denoted as WEBER-1, WEBER-3, and WEBER-5, respectively. The bitumen emulsion residue without waterborne epoxy resin was used as the control sample and denoted as WEBER-0.

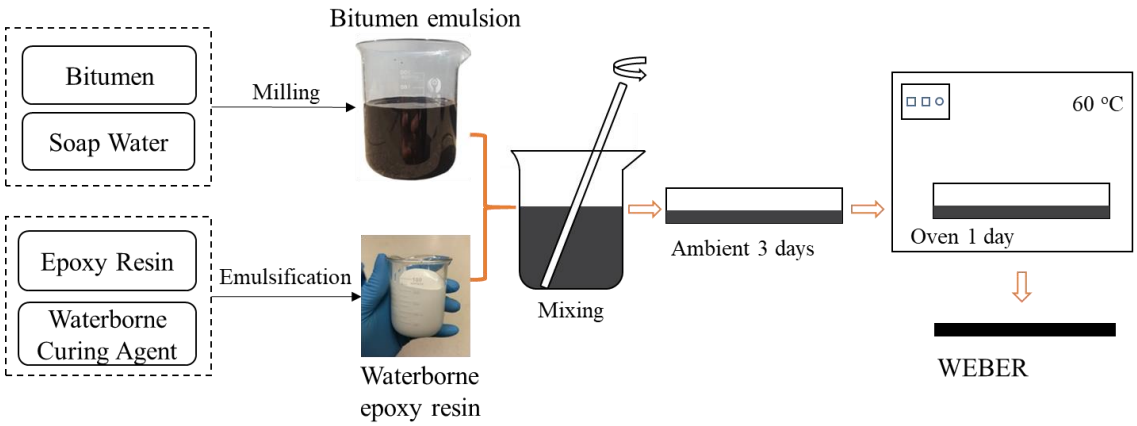

Figure 1 Procedure for preparing WEBER

Table 1 Properties of bitumen emulsion

Item		**Value**
Particle charge		Positive
Solid content (%)		63.0
Storage stability (%)	1 day	0.2
	5 day	2.8
Particle size (μm)	D10	3.956
	D50	8.039
	D90	42.305
	D[3,2]	5.169
Residual bitumen	Penetration (25 °C, 0.1 mm)	64.5
	Softening point (°C)	48.5
	Viscosity at 135 °C (mPa·s)	477.5

Note: D[3,2] represents the Sauter mean diameter, also known as Surface Area Moment Mean. It estimates the mean size of a given particle distribution, which is calculated from the following equation.

$$D[3,2] = \frac{\sum_{1}^{n} D_i^3 v_i}{\sum_{1}^{n} D_i^2 v_i} \quad (1)$$

where D_i is the diameter of the particle, and v_i is the probability density function of D_i size.

2.2 Experiments

Attenuated Total Reflection - Fourier Transform Infrared Spectroscopy

ATR-FTIR (Spectrum Two, PerkinElmer, Figure 2) was used to analyse the FTIR spectra of WEBERs with a 4 cm^{-1} resolution between 400 and 4,000 cm^{-1}. Each spectrum represents the accumulation of 32 scans. The ATR crystal used was ZnSe. The sample for the ATR-FTIR was prepared as follows. The crystal was first cleaned using dichloromethane, and a small amount of binder was attached on the crystal, which was then slightly pressed to ensure close contact between the sample and the crystal. During the test, the background spectrum was scanned in advance, the absorbance of the sample by ATR-FTIR was then measured, and the background spectrum was finally subtracted automatically. The spectra then went through a baseline correction to obtain the final spectra.

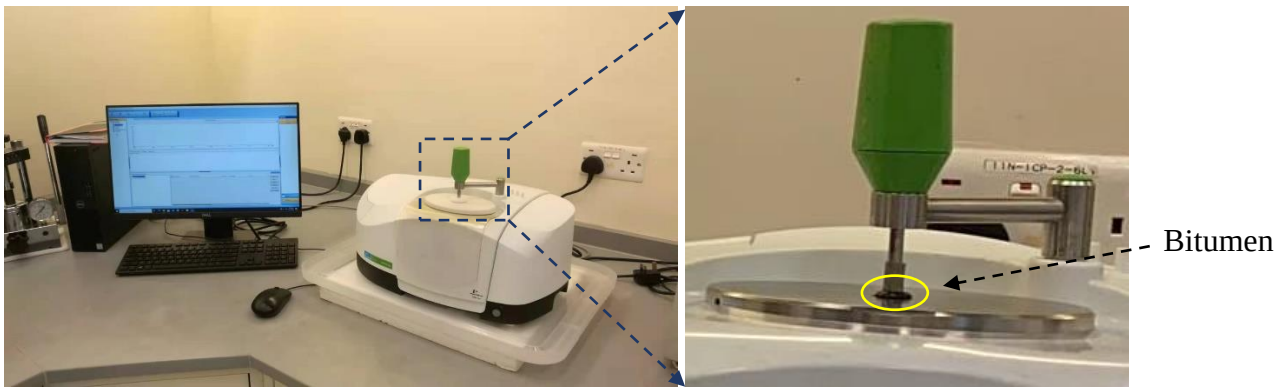

(a) (b)

Figure 2 (a) ATR-FTIR equipment setup and (b) sample preparation

Confocal Laser Scanning Microscopy (CLSM)

A Leica TCS SPE Confocal Microscope (Figure 3) was used to characterize the microstructure images of the specimens. The CLSM images were obtained from the focal plane with point-by-point laser scanning, any noise resulting from out of focus plane will be removed optically. Thus, the CLSM images symbolize the cross-section microstructure from the focal plane of the specimen. This technique can more authentically represent the microstructure of the materials compared with conventional widefield microscopy.

To prepare the sample, one drop of bitumen emulsion was placed on a glass slide, which was

dried at ambient room condition for 1-2 h, and a cover glass was put on top of the sample subsequently. The samples were then transferred into an oven and conditioned at 60 ºC for 4 h. In this process, the water in emulsion evaporates, and the waterborne epoxy resin cures at the same time. The images were recorded in the fluorescent mode activated by a laser with a wavelength of 488 nm (blue light). The acousto-optical tunable filter and Advanced Correction System (ACS) objectives were applied, and the photomultiplier tube (PMT) camera and LAS X Software were used during the measurement. After obtaining the images, no special visual manipulation was involved, except for the increase of the contrast between the epoxy phase and the bitumen phase to make it clearer (Figure 4).

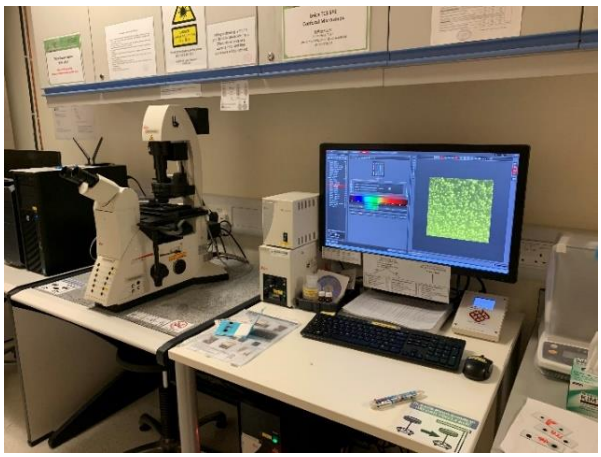

Figure 3 CLSM equipment setup

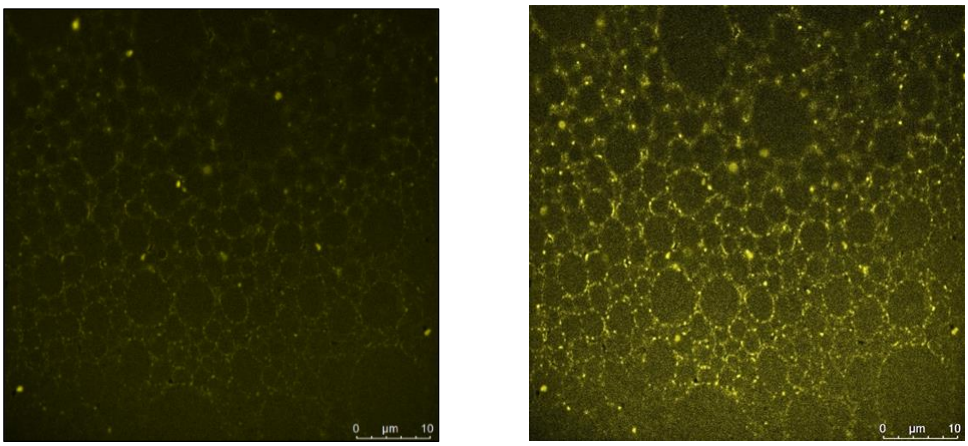

(a) (b)

Figure 4 CLSM images of WEBER-3 (a) original image, and (b) image with higher color contrast

Frequency Sweep Test

The bulk rheological properties of the WEBERs were tested employing a dynamic shear rheometer (DSR, MCR 702, Anton Paar) with the 8 mm parallel plates at a gap of 2 mm. Frequency sweep tests over the range of 0.1-30 Hz at the temperatures of -10 °C, 0 °C, 10 °C, 20 °C, 30 °C, 40 °C, 50 °C, and 60 °C were conducted in the linear viscoelastic domain on all specimens. The master curves of the complex modulus were then constructed using the time-temperature superposition principle at the reference temperature of 10 °C based on the Williams-Landel-Ferry (WLF) equation.

2.3 Model Description

To construct a master curve of the complex modulus, the experimental data obtained at different temperatures were shifted to a reference temperature according to the time-temperature superposition principle. Based on this principle, lower frequency corresponds to higher temperature, while higher frequency corresponds to lower temperature. The shift factors $\alpha(T)$ were calculated using the WLF equation (Williams et al., 1955),

$$\log a(T) = \frac{-C_1(T - T_r)}{C_2 + T - T_r} \tag{2}$$

where C_1 and C_2 are fitting parameters, T is the testing temperature (K), and T_r is the reference temperature (K).

The reduced frequency ω_r at the reference temperature was then calculated by the following equation,

$$\omega_r = \omega \times 10^{\log a(T)} \tag{3}$$

Figure 5 illustrates the '2S2P1D' model, which is the analogical model composed of 2 spring elements, 2 parabolic elements and 1 dashpot element (Olard and Di Benedetto, 2003).

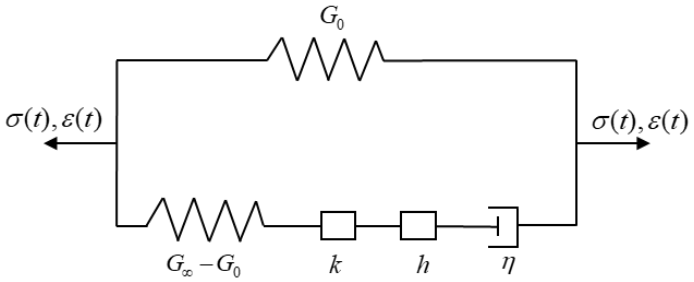

Figure 5 The '2S2P1D' model

The complex shear modulus G^* of the '2S2P1D' model is given as

$$G^*(\omega) = G_0 + \frac{G_g - G_0}{1 + \alpha(i\omega\tau)^{-k} + (i\omega\tau)^{-h} + (i\omega\beta\tau)^{-1}} \tag{4}$$

where ω is the frequency, k and h are the exponents for the parabolic elements with values between 0 and 1 (a smaller value corresponds to a more elastic element and a larger value corresponds to a more viscous element), α is a constant, G_0 is the static shear modulus when $\omega=0$, G_g is the glassy shear modulus when $\omega=\infty$, τ is the characteristic time influenced only by the temperature for a specific material, and β is a constant defined as

$$\eta = (G_g - G_0)\beta\tau \tag{5}$$

in which η is the Newtonian viscosity.

The master curves of the complex modulus fitted by the '2S2P1D' model were obtained through the regression analysis in the Excel spreadsheet, using Eq. (6) as the objective function.

$$f_{\min} = \sum \frac{|G'_M - G'_E|}{G'_E} + \sum \frac{|G''_M - G''_E|}{G''_E} + \sum \frac{|G^*_M - G^*_E|}{G^*_E} + \sum \frac{|\delta_M - \delta_E|}{\delta_E} \tag{6}$$

where G', G'', G^*, and δ denote the storage, loss, complex shear modulus, and phase angle, respectively. The subscripts M and E represent the data obtained from model and experiment, respectively.

3 Results and Discussions

3.1 Infrared Spectra of WEBERs

After waterborne epoxy resin emulsion was mixed with bitumen emulsion, the cross-link curing reaction would proceed as water evaporates. Figure 6 demonstrates the FTIR spectra of all the WEBERs. As the dosages of waterborne epoxy resin were small, no significant difference between the WEBERs was observed. However, a close look at the fingerprint region reveals that the peak intensity at 1,250 cm^{-1} corresponding to the ether group (C-O-C) in the epoxy resin increased with increasing contents of waterborne epoxy resin. This outcome is consistent with the amount of waterborne epoxy resin added into bitumen emulsion.

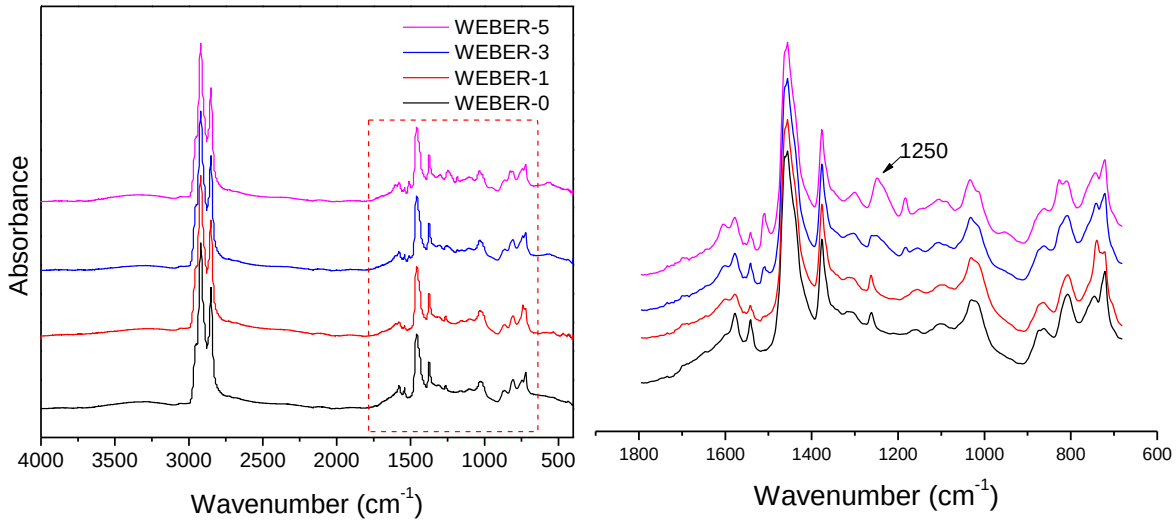

(a) (b)

Figure 6 (a) Infrared spectra of WEBERs and (b) the details in the fingerprint region

In an attempt to quantitatively evaluate the ether group in WEBERs, the ether group intensity can be calculated as follows,

$$I_{C-O-C} = \frac{A_{C-O-C}}{A_{ref}} \cdot 100\% \quad (7)$$

where A_{C-O-C} and A_{ref} are the peak area of ether group (C-O-C) and the area sum of the peak at 2924 and 2852, corresponding to the stretching vibration of aliphatic groups (CH_2 and CH_3).

The intensities of the ether group are presented in Table 2. It is clear that the ether group area increased continuously with larger concentration of waterborne epoxy resin, indicating the homogeneous of WEBERs.

Table 2 Comparison of the ether group intensity of WEBERs

Sample ID	$I_{C\text{-}O\text{-}C}$ (%)
WEBER-0	0.46
WEBER-1	0.55
WEBER-3	1.56
WEBER-5	3.14

3.2 Microstructure Images of WEBERs

Figure 7 demonstrates the fluorescence images of the cured WEBERs. The dark phase and the yellow phase represent bitumen and epoxy resin networks, respectively. It can be noticed that the cured epoxy resin formed an inter-connected polymer (or honeycomb-like) structure around the bitumen phase when the concentration of waterborne epoxy resin reached 3wt%. In contrast, a study by Liu et al. (Liu et al., 2018) used a commercial waterborne epoxy resin to modify bitumen emulsion, and such polymer-rich film structure was not observed even when 40wt% waterborne epoxy resin was added. Gu et al. (Gu et al., 2019) evaluated the microstructure of a non-ionic based waterborne epoxy resin modified bitumen emulsion using the fluorescence microscopy and scanning electrical microscopy (SEM). Their findings indicated that the polymer-rich film structure could only be formed with the content of the waterborne epoxy resin larger than 20wt%. The difference of the microstructure images between this study and the previous studies might be due to the different compositions of the waterborne epoxy resin, which leads to different compatibility of the waterborne epoxy resin

with bitumen emulsion.

After being mixed with bitumen emulsion, the waterborne epoxy resin distributed in the water phase at first. With the evaporation of water and the curing of waterborne epoxy resin, the inter-connected epoxy resin film was formed around the bitumen phase. It is worth noting that the size of most of the dispersed bitumen phase was smaller than 10 μm in the microstructures of WEBER-3 and WEBER-5, which were close to their original sizes before breaking. Such inter-connected epoxy structure may dramatically change the viscoelastic performance of the emulsion residues, which will be further discussed in the following parts of this paper.

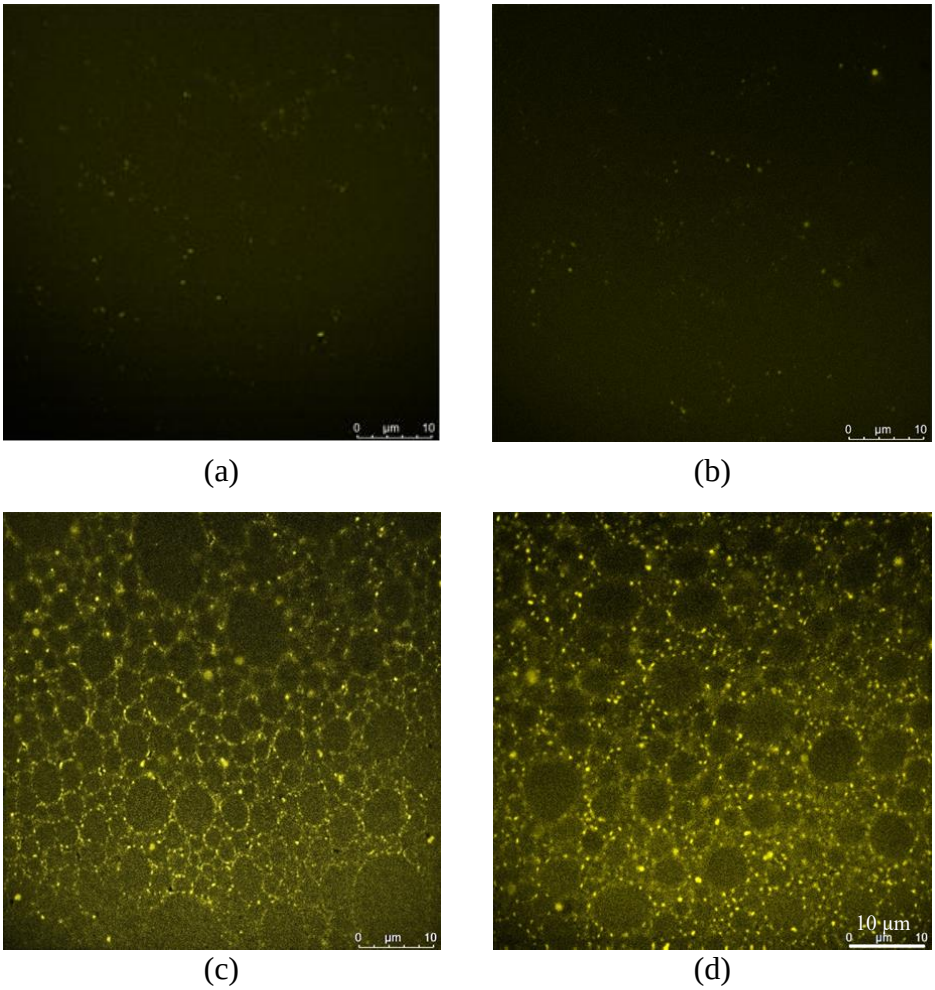

(a) (b)

(c) (d)

Figure 7 CLSM images of WEBERs (a) WEBER-0, (b) WEBER-1, (c) WEBER-3, and (d) WEBER-5 (scale bar: 10 μm)

3.3 Constitutive Modelling Results

Figure 8 illustrates the master curves of the modulus ($|G^*|$) and the phase angle (δ) for all the WEBERs at the reference temperature of 10 °C. As shown in Figure 8(a), the $|G^*|$ values for all emulsion residues were close to 10^9 Pa at higher frequency, while larger quantities of waterborne epoxy resin led to significant improvement of $|G^*|$ at lower frequency. This result indicated that the addition of waterborne epoxy substantially decreased the temperature susceptibility of the WEBERs. On the other hand, the phase angle master curves showed a reverse trend, revealing that the waterborne epoxy resin increased the elasticity of the emulsion residues. It is worth noting that the phase angle of WEBER-0 approached 90° at lower frequency, demonstrating Newtonian liquid response at high temperature. What stands out in the figure is that the phase angles of WEBER-3 and WEBER-5 first increased and then decreased with decreasing frequency. Such phenomenon is typically associated with the presence of inter-connected polymer-rich phase that resulted from the phase separation of the polymer in the bitumen matrix (Polacco et al., 2006, Xia et al., 2016). This result is consistent with the microstructure images shown in Figure 7. It is also noticeable that the phase angles of WEBER-5 were always smaller than 45°, indicating that WEBER-5 had elastic-dominated response within the whole frequency range. A deviation from the smooth phase angle mater curves was observed with larger concentration of waterborne epoxy resin, especially for WEBER-5. Such phenomenon is commonly seen for the polymer modified bitumen binders (Md. Yusoff et al., 2013, Saboo and Kumar, 2016), which indicates the limitation of the time-temperature superposition principle.

The fluorescence microscopy test results have shown the inter-connected epoxy resin structures in WEBER-3 and WEBER-5. Such distinct structures significantly improved the elasticity of the emulsion residues. At very low temperature (high frequency), the bitumen is very stiff, and the overall performance of the WEBERs is dominated by the bitumen, thus the

difference among different WEBERs was insignificant. When the temperature started to increase, both the bitumen and the polymer structure softened to some extent, leading to larger phase angle. With the further increase of temperature, the bitumen transferred to a viscous state. However, the polymer structure did not melt at this stage, and the overall performance of the mixture was dominated by the epoxy resin networks. As a result, the phase angle decreased at higher temperature (lower frequency).

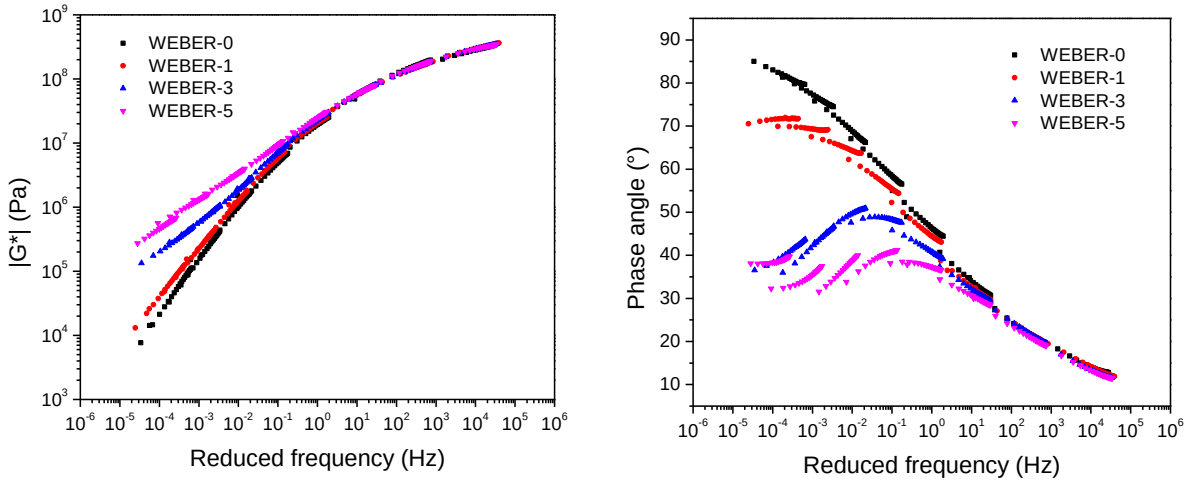

(a) (b)

Figure 8 Master curves of (a) complex moduli and (b) phase angles at the reference temperature of 10 °C

Figure 9 presents the fitting outcome of the master curves of complex modulus by the '2S2P1D' model. It can be seen that both the modulus and the phase angle data can be well fitted by the '2S2P1D' model. Table 3 and Table 4 present the fitting parameters for the WLF function that determines the horizontal shifting factors, and the parameters for the '2S2P1D' model, respectively. The coefficients of determination, R^2, are larger than 0.96 for all cases as demonstrated in Table 5.

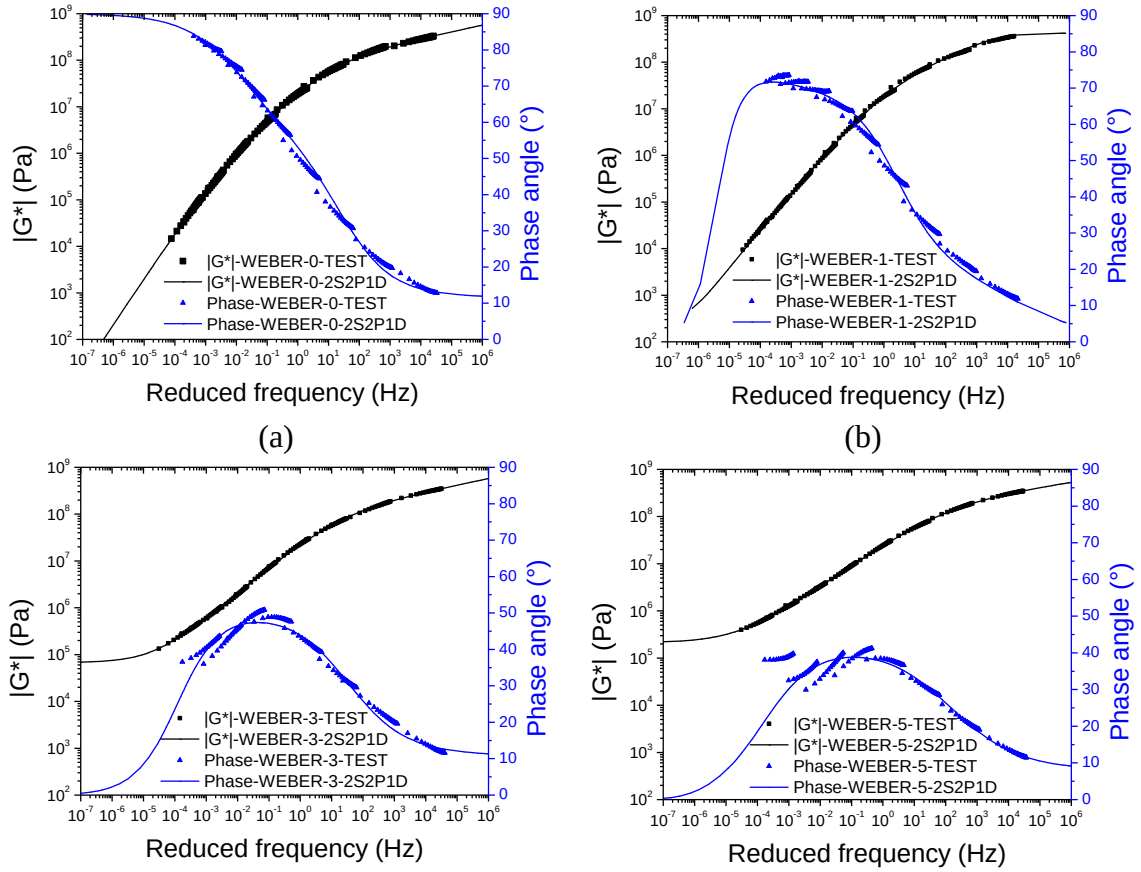

Figure 9 Master curves of complex moduli and phase angles (reference temperature: 10 °C): (a) WEBER-0, (b) WEBER-1, (c) WEBER-3, (d) WEBER-5

Table 3 Parameters for WLF equation

Sample ID	C_1	C_2 (K)
WEBER-0	16.97	134.03
WEBER-1	19.51	163.10
WEBER-3	17.50	135.79
WEBER-5	22.36	172.94

Table 4 '2S2P1D' model parameters for WEBERs

Sample ID	*k*	*h*	*α*	*β*	*τ (s)*	*G_0 (Pa)*	*G_g(Pa)*
WEBER-0	0.138	0.600	31.1	4.57E+02	4.68E-05	7.50E-09	9.97E+09

WEBER-1	0.270	0.758	4.7	7.96E+01	4.32E-02	3.12E+02	3.57E+08
WEBER-3	0.132	0.558	21.8	4.94E+05	4.77E-05	6.75E+04	7.13E+09
WEBER-5	0.097	0.466	22.6	4.94E+06	2.89E-06	2.19E+05	1.06E+10

Table 5 Fitting quality of the experiment data (R^2 values)

Sample ID	R^2-Complex modulus	R^2-Phase angle
WEBER-0	0.984	0.987
WEBER-1	0.997	0.991
WEBER-3	0.999	0.972
WEBER-5	0.999	0.969

3.4 Relation Between Microstructure and Viscoelastic Behavior

It can be noticed from Table 4 that G_0 of the pure bitumen emulsion residue WEBER-0 was close to 0, indicating that the stand-alone spring can be removed from the '2S2P1D' model for WEBER-0. Comparing the parameters of the three emulsion residues containing waterborne epoxy resin, i.e., WEBER-1, WEBER-3, and WEBER-5, it can be found that both the glassy spring parameter G_g and the static stand-alone spring parameter G_0 increased with larger concentration of waterborne epoxy resin, indicating increased elasticity of the binder. In contrast, the parabolic element parameters *k* and *h* decreased with larger concentration of waterborne epoxy resin, suggesting denser epoxy resin networks have been formed in the emulsion residue. In addition, the value of *h* was over three times larger than that of *k* for each specimen, which revealed that the first parabolic element performed more like an elastic spring. It can be further noticed that the parameter α increased with increasing concentration of waterborne epoxy resin. Previous studies (Olard et al., 2003, Md. Yusoff et al., 2013) have shown that α becomes larger for stiffer binders, which is consistent with the findings of this

study, as larger concentration of waterborne epoxy resin leads to higher stiffness. Furthermore, the parameter β is related to the viscous characteristic of the linear dashpot, which showed an increasing trend with the increase of waterborne epoxy resin concentration, because of the increment of viscosity.

Figure 10 illustrates the proposed relationship between the parameters of the '2S2P1D' model and the microstructure of WEBER. The cured epoxy resin film forms the skeleton structure of the material, and the dispersed bitumen phase is encapsulated by the epoxy resin film. The skeleton epoxy resin film can be represented by the stand-alone static spring, which provides the elasticity to the material. On the other hand, the interaction between the epoxy resin film and bitumen phase are represented by the parabolic elements. When a stress in the linear viscoelastic domain is applied on the material, an instant deformation will appear because of the elastic epoxy resin film, which increases with time due to the viscoelasticity (Li et al., 2021). Upon removing the stress, an instant elastic recovery will occur, followed by a slow deformation recovery with the increase of time. Given the viscous characteristic of the bitumen phase, part of the deformation may not be recovered.

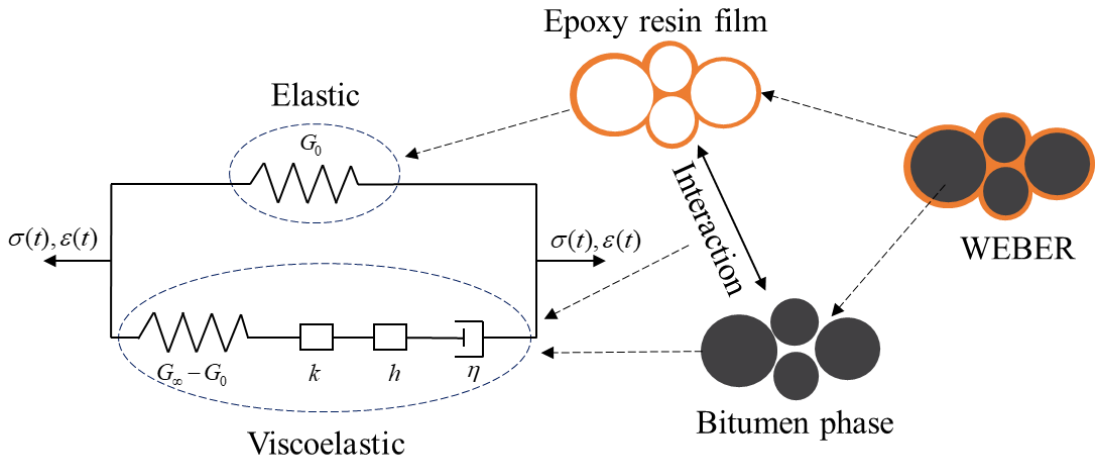

Figure 10 Schematic relation between the microstructure of WEBER and the '2S2P1D' model

4 Summary

In this study, the infrared spectra of WEBER were first characterized. The microstructure and viscoelastic behavior of the WEBER, as well as their relationship were then investigated. The following findings have been obtained based on the outcomes of this study:

- The fluorescence microscopy images revealed that the cured waterborne epoxy resin formed a homogeneous inter-connected polymer-rich film around the bitumen phase when the waterborne epoxy resin concentration reached 3wt%.
- The '2S2P1D' model can well describe the viscoelastic response of WEBER.
- The microstructure of the WEBER is closely related with the parameters of the '2S2P1D' model. Both the glassy modulus parameter G_g and the static modulus G_0 increased with increasing waterborne epoxy resin contents, while the parabolic parameters k and h decreased.

Overall, the findings from this study suggest that the waterborne epoxy resin can form the inter-connected film structure around the bitumen phase in WEBER, which significantly changed the viscoelastic behavior of the bitumen emulsion residue. Nevertheless, it is worth noting that the waterborne epoxy resin used in this study was custom-prepared in lab, and its distinct molecular structure resulted in the findings of this study. The molecular structures of the commercially available waterborne epoxy resins, however, are usually unknown to the users, and can be different from the waterborne epoxy resin in the present research. Thus, the effects of different commercial waterborne epoxy resins on bitumen emulsion should be investigated in future studies.

Acknowledgements

The authors would like to acknowledge the funding support from the Hong Kong Innovation

and Technology Commission through the Guangdong-Hong Kong Technology Cooperation Funding Scheme (TCFS) project GHP/116/18GD.

Data availability statement

The data of this study are available upon request.

References

CALABI-FLOODY, A. & THENOUX, G. 2012. Controlling asphalt aging by inclusion of byproducts from red wine industry. *Construction and Building Materials,* 28**,** 616-623.

CAPITÃO, S. D., PICADO-SANTOS, L. G. & MARTINHO, F. 2012. Pavement engineering materials: Review on the use of warm-mix asphalt. *Construction and Building Materials,* 36**,** 1016-1024.

DĘBSKA, B. & LICHOŁAI, L. 2016. The effect of the type of curing agent on selected properties of epoxy mortar modified with PET glycolisate. *Construction and Building Materials,* 124**,** 11-19.

EDWARDS, Y., TASDEMIR, Y. & ISACSSON, U. 2005. Influence of Commercial Waxes on Bitumen Aging Properties. *Energy & Fuels,* 19**,** 2519-2525.

FORBES, A., HAVERKAMP, R. G., ROBERTSON, T., BRYANT, J. & BEARSLEY, S. 2001. Studies of the microstructure of polymer-modified bitumen emulsions using confocal laser scanning microscopy. *Journal of Microscopy,* 204**,** 252-257.

GÓMEZ-MEIJIDE, B. & PÉREZ, I. 2014. A proposed methodology for the global study of the mechanical properties of cold asphalt mixtures. *Materials & Design,* 57**,** 520-527.

GU, Y., TANG, B., HE, L., YANG, F., WANG, H. & LING, J. 2019. Compatibility of cured phase-inversion waterborne epoxy resin emulsified asphalt. *Construction and Building Materials,* 229**,** 116942.

HU, C., ZHAO, J., LENG, Z., PARTL, M. N. & LI, R. 2019. Laboratory evaluation of waterborne epoxy bitumen emulsion for pavement preventative maintenance application. *Construction and Building Materials,* 197**,** 220-227.

HUET, C. 1965. *Etude par une méthode d'impédance du comportement viscoélastique des matériaux hydrocarbonés.*

JIANG, J., NI, F., ZHENG, J., HAN, Y. & ZHAO, X. 2020. Improving the high-temperature performance of cold recycled mixtures by polymer-modified asphalt emulsion. *International Journal of Pavement Engineering,* 21**,** 41-48.

KHADIVAR, A. & KAVUSSI, A. 2013. Rheological characteristics of SBR and NR polymer modified bitumen emulsions at average pavement temperatures. *Construction and Building Materials,* 47**,** 1099-1105.

KIM, Y.-R. & LEE, H.-J. 2003. Evaluation of the effect of aging on mechanical and fatigue properties of sand asphalt mixtures. *KSCE Journal of Civil Engineering,* 7**,** 389-398.

LI, R., LENG, Z., PARTL, M. N. & RAAB, C. 2021. Characterization and modelling of creep and recovery behaviour of waterborne epoxy resin modified bitumen emulsion. *Materials and Structures,* 54**,** 8.

LI, R., LENG, Z., WANG, Y. & ZOU, F. 2020. Characterization and correlation analysis of mechanical properties and electrical resistance of asphalt emulsion cold-mix asphalt. *Construction and Building Materials,* 263**,** 119974.

LI, R., LENG, Z., ZHANG, Y. & MA, X. 2019. Preparation and characterization of waterborne epoxy modified bitumen emulsion as a potential high-performance cold binder. *Journal of Cleaner Production,* 235**,** 1265-1275.

LIU, M., HAN, S., PAN, J. & REN, W. 2018. Study on cohesion performance of waterborne epoxy resin emulsified asphalt as interlayer materials. *Construction and Building Materials,* 177**,** 72-82.
LU, X. & ISACSSON, U. 2000. Artificial aging of polymer modified bitumens. *Journal of Applied Polymer Science,* 76**,** 1811-1824.
MD. YUSOFF, N. I., MOUNIER, D., MARC-STÉPHANE, G., ROSLI HAININ, M., AIREY, G. D. & DI BENEDETTO, H. 2013. Modelling the rheological properties of bituminous binders using the 2S2P1D Model. *Construction and Building Materials,* 38**,** 395-406.
MIRWALD, J., MASCHAUER, D., HOFKO, B. & GROTHE, H. 2020. Impact of reactive oxygen species on bitumen aging – The Viennese binder aging method. *Construction and Building Materials,* 257**,** 119495.
NIVITHA, M. R., PRASAD, E. & KRISHNAN, J. M. 2016. Ageing in modified bitumen using FTIR spectroscopy. *International Journal of Pavement Engineering,* 17**,** 565-577.
OLARD, F. & DI BENEDETTO, H. 2003. General '2S2P1D' Model and Relation Between the Linear Viscoelastic Behaviours of Bituminous Binders and Mixes. *Road Materials and Pavement Design,* 4**,** 185-224.
OLARD, F., DI BENEDETTO, H., ECKMANN, B. & TRIQUIGNEAUX, J.-P. 2003. Linear Viscoelastic Properties of Bituminous Binders and Mixtures at Low and Intermediate Temperatures. *Road Materials and Pavement Design,* 4**,** 77-107.
POLACCO, G., STASTNA, J., BIONDI, D. & ZANZOTTO, L. 2006. Relation between polymer architecture and nonlinear viscoelastic behavior of modified asphalts. *Current Opinion in Colloid & Interface Science,* 11**,** 230-245.
RAAD, L., SABOUNDJIAN, S. & MINASSIAN, G. 2001. Field Aging Effects on Fatigue of Asphalt Concrete and Asphalt-Rubber Concrete. *Transportation Research Record,* 1767**,** 126-134.
SABOO, N. & KUMAR, P. 2016. Use of flow properties for rheological modeling of bitumen. *International Journal of Pavement Research and Technology,* 9**,** 63-72.
SAYEGH, G. Viscoelastic properties of bituminous mixtures. Intl Conf Struct Design Asphalt Pvmts, 1967.
TAKAMURA, K. Microsurfacing with SBR latex modified asphalt emulsion. 2002 Charlotte, NC, BASF.
TOPAL, A. 2010. Evaluation of the properties and microstructure of plastomeric polymer modified bitumens. *Fuel Processing Technology,* 91**,** 45-51.
WILLIAMS, M. L., LANDEL, R. F. & FERRY, J. D. 1955. The temperature dependence of relaxation mechanisms in amorphous polymers and other glass-forming liquids. *Journal of the American Chemical society,* 77**,** 3701-3707.
XIA, T., XU, J., HUANG, T., HE, J., ZHANG, Y., GUO, J. & LI, Y. 2016. Viscoelastic phase behavior in SBS modified bitumen studied by morphology evolution and viscoelasticity change. *Construction and Building Materials,* 105**,** 589-594.
YAMASAKI, H. & MORITA, S. 2014. Identification of the epoxy curing mechanism under isothermal conditions by thermal analysis and infrared spectroscopy. *Journal of Molecular Structure,* 1069**,** 164-170.
ZHU, J., BALIEU, R., LU, X. & KRINGOS, N. 2018. Microstructure evaluation of polymer-modified bitumen by image analysis using two-dimensional fast Fourier transform. *Materials & Design,* 137**,** 164-175.